PROTOPAPPAS, E., SMAL, C. A., and DE LANGE, F. G. Mechanical properties of a 316L forging material modified for resistance to sensitization. *INFACON 6. Proceedings of the 1st International Chromium Steel and Alloys Congress, Cape Town.* Volume 2. Johannesburg, SAIMM, 1992. pp. 97–103.

Mechanical Properties of a 316L Forging Material Modified for Resistance to Sensitization

E. PROTOPAPPAS, C. A. SMAL, and F. G. DE LANGE
AEC of South Africa, Pretoria, South Africa

When types 304 and 316 stainless steels are specified for structural and piping appliations in nuclear reactors, the susceptibility to intergranular stress–corrosion cracking (IGSCC) must be considered. When exposed in the sensitized condition to high-purity aqueous media containing dissolved oxygen and low chloride levels (less than 2 p.p.m.), premature failure can occur. Increased amounts of cold work, sensitization, loading in the transverse direction, and compositional heterogeneities will decrease the time to failure at a specific load.

AEC of South Africa has manufactured a 316L nuclear-grade stainless steel that eliminates the problem of IGSCC. Apart from having a low content of undesirable trace elements, resistance to sensitization is improved considerably when compared with the usual 316L available on the market.

This paper describes the characterization of the alloy. The results include chemical analyses, mechanical properties, environmental fatigue, fractography, metallography, and resistance to sensitization.

Introduction

Austenitic stainless steels can be made more susceptible to stress–corrosion cracking (SCC) in high-purity aqueous media at high temperature (300 °C) if the steels have been sensitized by slow cooling through the temperature range 550 to 850 °C, for instance during welding and stress-relief cycles. SCC attack in sensitized material occurs by a mechanism of intergranular failure, and is aggravated by the precipitation of carbides, the depletion of alloy, and the segregation of impurities at the grain boundaries. Intergranular attack can occur in the presence of an aqueous solution, and evidence of such attack has been noted in nuclear-reactor environments.

In an effort to mitigate this effect, nuclear-grade austenitic stainless steels have been developed by steelmakers worldwide. A similar 316 nuclear-grade steel has been manufactured by AEC of South Africa. This paper describes the microstructure, and the mechanical and SCC properties that have been established to date for this steel (AEC-316LNG).

Modified 316L Stainless Steel

Chemical Composition

A comparison of the chemical specification for AEC-316LNG steel with that for previously utilized 316L grade steels is given in Table I. In order to improve the resistance to sensitization, the carbon content of the AEC steel is limited to 0,02 per cent maximum. The expected loss of strength due to the lower carbon content is compensated for by the addition of nitrogen up to a limit of 0,12 per cent. The combined interstitial content of the carbon and nitrogen is limited to 0,13 per cent in order to increase its resistance to irradiation-induced sensitization.

TABLE I
COMPARISON OF CHEMICAL COMPOSITION

Element	316L	AEC-316LNG as specified	AEC as cast
Carbon	0,03 max.	0,02 max.	0,016
Manganese	2,0 max.	2,0 max.	1,05
Silicon	1,0 max.	0,75 max.	0,55
Sulphur	0,03 max.	0,01 max.	0,009
Phosphorus	0,03 max.	0,03 max.	0,022
Chromium	16-18	16-18	16,6
Nickel	10-14	10-14	10,4
Molybdenum	2-3	2-3	2,02
Nitrogen	–	0,12 max.	0,021
Boron	–	0,004 max.	<0,001
Cobalt	–	0,05 max.	0,036

The sulphur content was lowered to a maximum of 0,01 per cent in order to reduce the content of deleterious inclusions. This can influence the initiation behaviour of ductile fracture. However, too low a sulphur content has adverse effects on welding behaviour owing to reduced arc-penetration characteristics.

Cobalt was limited to a maximum of 0,05 per cent, thereby minimizing undesirable radiation effects due to the (n, γ) reaction. Cobalt is normally added to improve hot-working properties.

Boron was limited to 0,004 per cent maximum because of its neutron-capture properties, which affect the neutron economy adversely.

Manufacturing Procedure

A 32 t cast of AEC-316LNG was manufactured by the vacuum oxygen decarburization (VOD) process. Further refinement was done by Electroslag Remelting (ESR). A reduction ratio of 3 was effected through forging, and the steel was subsequently solution-annealed at 1050 °C, followed by quenching in water.

Material Properties

The material properties of the forged 316LNG, as compared with the specified AEC requirements, are shown in Table II.

TABLE II
PROPERTIES OF FORGED STEEL

Parameter	AEC specification	Result
Ultrasonic inspection	ASME III NB-2542	No indications
Dye-penetrant inspection	ASME III NB-2546	No indications
Intergranular attack	ASTM A 262 Pr. E	Acceptable
Tensile strength	515 MPa min.	526 MPa min.
Yield strength	205 MPa min.	246 MPa min.
Elongation	30% min.	70% min.
Reduction in area	40% min.	85% min.
Tensile strength (350 °C)	425 MPa min.*	400 MPa min.
Yield strength (350 °C)	101 MPa min.*	220 MPa min.
Charpy impact energy (20 °C)	55 J min.	270 J min.
Hardness	95 HRB max.	90 HRB
ASTM grain size	< 4 recommended	2–4

* For information only—not acceptance criteria

Sensitization Behaviour

The ASTM A-262 Practice E screening test for sensitization was satisfied by the AEC steel. However, Atteridge[1] has demonstrated that very-low-carbon steels can be sensitized at higher temperatures and longer exposure times than the sensitization heat treatment prescribed in ASTM A-262. Accordingly, two further heat treatments that had been shown to induce senzitization in very-low-carbon 316 steels[1] were carried out. These were isothermal treatments at 700 °C for 8 and 100 hours respectively.

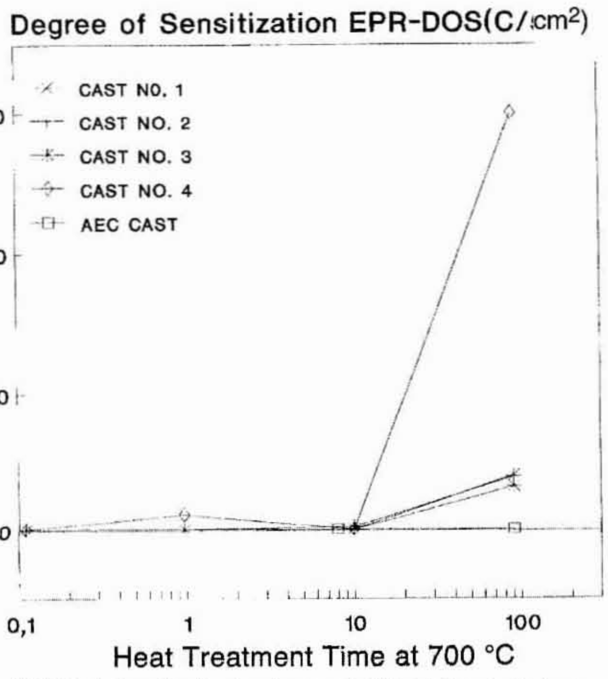

FIGURE 1. Sensitization development in 316 stainless steels due to heat treatment at 700 °C

Chemical Composition, %				
Cast	C	Ni	Mo	Cr
No 1	0,011	12,7	2,1	17,7
No 2	0,012	12,6	2,2	17,8
No 3	0,013	12,7	2,1	17,1
No 4	0,015	12,9	2,3	16,8
AEC	0,016	10,4	2,0	16,6

The sensitization behaviour of the specimens was evaluated by electrochemical potentiokinetic reactivation (EPR) tests[2]. Atteridge *et al.*[1] regard a degree of sensitization (DOS) greater than 20 C/cm^2, after an allowance has been made for grain-size effects, as 'severely sensitized'. The maximum DOS allowable for nuclear piping applications is fixed at a maximum of 2 C/cm^2, where the area under consideration is the effective chromium-depleted grain-boundary area[3]. For the AEC-316LNG steel, zero values were obtained for both the above heat treatments.

Figure 1 compares these values with those developed by Atteridge *et al.*[1] for low-carbon 316 steels. It shows that the resistance to sensitization of the AEC-316LNG is extremely high, which is consistent with the analyses of grain boundaries by scanning-transmission electron microscopy (STEM), which confirmed that no grain-boundary precipitation or chromium depletion had occurred. It should be noted that this behaviour is not in keeping with the trends shown by Atteridge (Figure 1) and that the material is therefore being examined further.

Fatigue Behaviour

The fatigue tests on AEC-316LNG were conducted mainly on solution-annealed material. A limited number of tests were performed on samples heat-treated at 700 °C for 8 hours. Both the fatigue-crack initiation and the propagation characteristics of the steel were investigated. Testing involved sinusoidal loading of compact tension specimens with a notch in the LC orientation (ASTM notation). The following test variables were used:

- R ratios between 0,1 and 0,8
- Temperatures of 20 °C and 290 °C
- Environments of air and water.

The R ratio (or stress ratio) is defined as the ratio of minimum to maximum stress. Crack initiation and subsequent

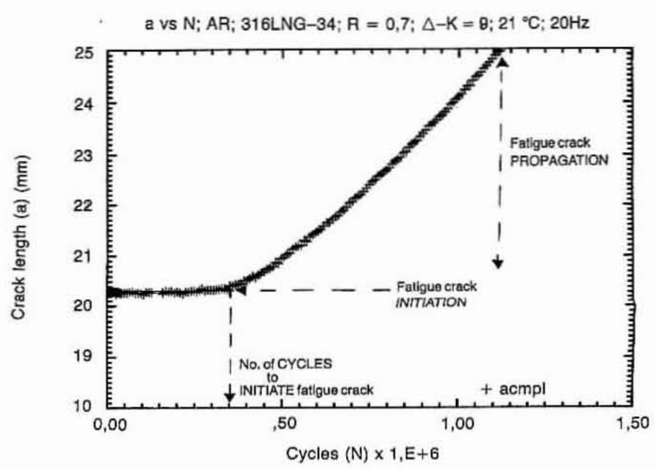

FIGURE 2. Initiation and propagation of a fatigue crack

crack propagation were determined by standard compliance techniques. The equipment used is capable of determining differences in crack length of 0,1 mm.

In the present work, the 'apparent' initiation threshold is defined by the stress-intensity level where there is no deviation from the original crack length in approximately 2 million cycles. This definition of initiation is as illustrated in Figure 2, and is in keeping with that of Devaux *et al.*[4] and Saainouni and Bathias[5]. In both these cases and the present work, initiation was verified metallographically.

Initiation of Fatigue Cracks

Initiation results are given as a function of ΔK in Figures 3 to 6. The use of this parameter is justified by the very sharp notch-tip root radius of 0,1 mm that was used in this work. The limiting notch-tip radius, where no further effects on initiation are evident, is in the region 0,2 to 0,25 mm, and has been determined by a number of authors[4-8] for a wide variety of steels ranging from mild to stainless steel.

The tests on solution-annealed and 'sensitized' material at room temperature and at an applied R ratio of 0,1 are given in Figure 3, and are compared with published data for various 316 stainless steels[4,5,11]. Good agreement was found between the 316LNG steel and other 316 steels.

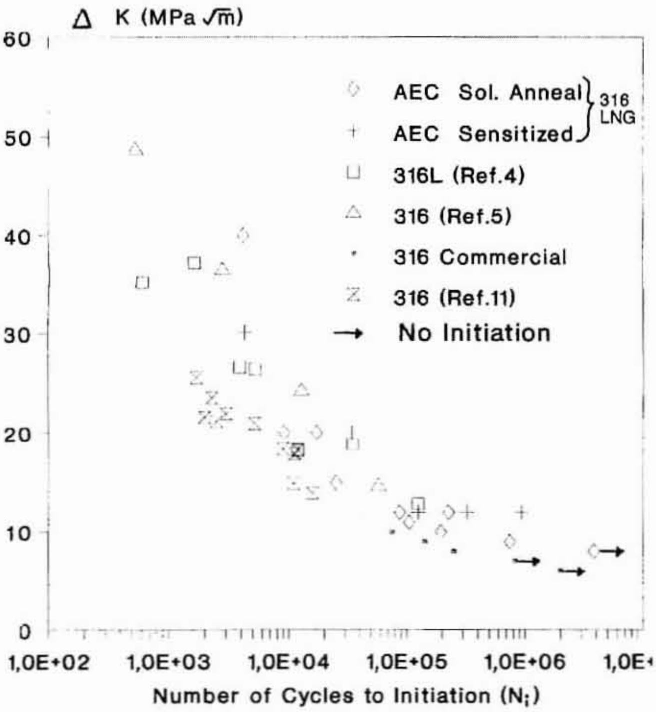

FIGURE 3. Initiation behaviour of various stainless steels in air (20 °C, $R = 0,1$)

The 'apparent' initiation threshold for the solution-treated material is at approximately $\Delta K = 8$ MPa$\sqrt{m}$. It appears that the 'sensitized' material has marginally better resistance to initiation than its solution-treated counterpart. Further testing is under way.

Effect of R ratio

The effect of the applied R ratio on the initiation behaviour of the solution-treated material at 20 °C is given in Figure 4. R ratios in the range 0,1 to 0,8 do not display significantly different initiation values. The only significant difference

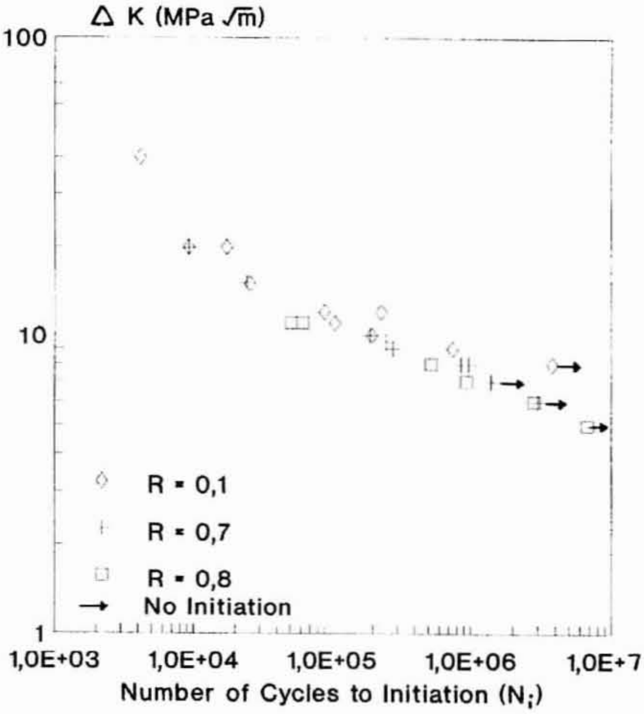

FIGURE 4. Effect of R-ratio upon initiation. (AEC 316LNG, air, 20 °C, 20 Hz)

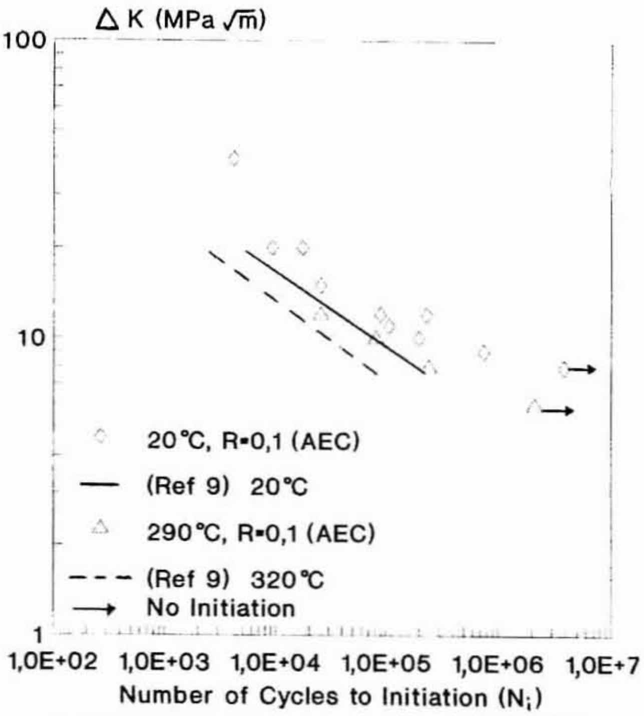

FIGURE 5. Effect of temperature on initiation (AEC-316LNG)

is seen in the levels of apparent thresholds obtained. These show a reduction in initiation threshold with increasing R ratio. The apparent threshold values are $\Delta K_T = 8$; 7; and 6 MPa$\sqrt{m}$ for $R = 0,1$; 0,7; and 0,8 respectively.

Influence of test temperature

The influence of test temperature is shown in Figures 5 and 6 for tests conducted at $R = 0,1$ and 0,6 respectively. For $R = 0,1$, there is an apparent reduction in initiation life of

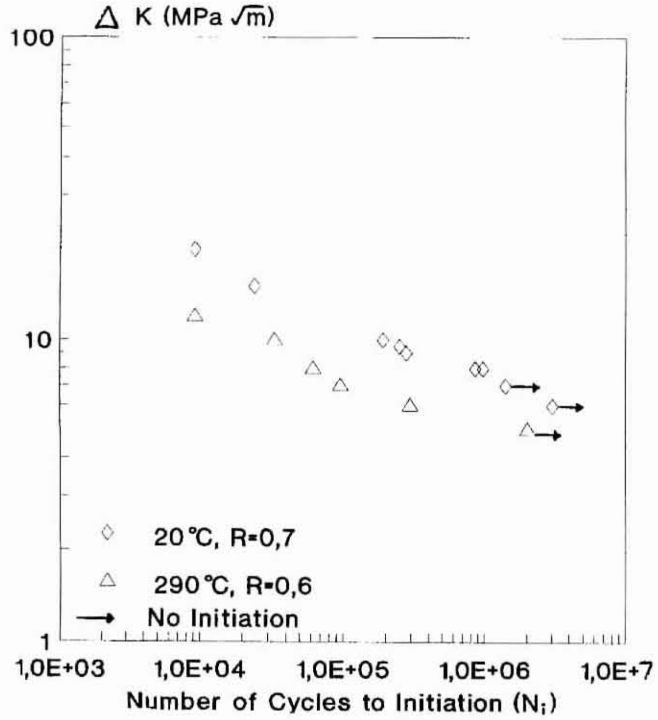

FIGURE 6. Effect of temperature on initiation (AEC-316LNG)

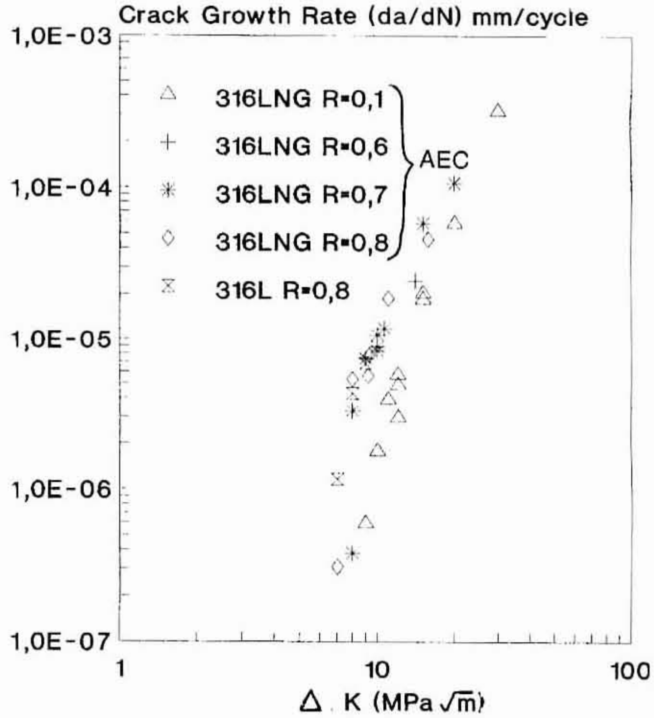

FIGURE 7. Effect of R ratio on crack growth (air, 20 °C, 20 Hz)

nearly a factor of 2 owing to an increase in temperature from 20 to 290 °C. Such a reduction is consistent with observations by D'Escatha *et al.* [9] for 316 and CF-8M steels at 20 and 320 °C (Figure 5).

Figure 6 shows that a further reduction in initiation life is observed at 290 °C, where R is increased from 0,1 to 0,6 or 0,7. At 290 °C, the number of cycles to the initiation of cracking is about ten times lower than the equivalent results at room temperature (Figure 6). The initiation threshold for R = 0,6 and T = 290 °C is about 5 MPa$\sqrt{m}$, which represents a reduction of 2 MPa$\sqrt{m}$ from that measured at 20 °C.

Propagation of Cracks

The crack-propagation rates developed after initiation are given in Figures 7 to 9. In each case, each point represents a single test conducted at constant ΔK. The propagation rate was established from several millimetres of growth (Figure 2).

Effect of R ratio

The test results conducted at 20 °C are summarized in Figure 7, where it can be seen that growth rates, at cyclic stress intensities within the range 8 to 20 MPa$\sqrt{m}$ for tests conducted at $0,6 < R < 0,8$, are similar. The average stage II growth rates in the form of the Paris–Erdogan law are given in Table III.

TABLE III
STAGE II GROWTH RATES*

Temp (°C)	R ratio	m	C
20	0,1	3,83	$3,6 \times 10^{-10}$
20	0,6; 0,7; 0,8	3,66	$2,2 \times 10^{-9}$
290	0,1	2,11	$6,5 \times 10^{-8}$
290	0,6	1,92	$1,6 \times 10^{-7}$

* $da/dN = C(\Delta K)^m$

From this table, it can be seen that an increase in temperature from 20 to 290 °C results in a decrease in the gradient or m constant by a factor of approximately 2 for both low and high R ratios. The effect of increasing the R ratio at a particular temperature does not significantly affect the gradient. Table III also shows that the C constant is dependent on both the R ratio and the temperature. At 20 °C, for the low R ratio (R = 0,1), C is about six times lower than for the high R ratios (R = 0,6; 0,7; 0,8). At 290 °C, the C constant for the lower R ratio is about 2,5 times less than for the higher R ratio (R = 0,6). However, temperature has a substantially larger effect on the C values obtained. For instance, for R = 0,1 an increase in the temperature from 20 to 290 °C increases the C constant by approximately 180 times. Similarly, for the higher R ratio, an increase in temperature increases the C value by approximately 75 times.

The values for an R ratio of 0,1 are lower than for the high R ratio at levels below about 30 MPa$\sqrt{m}$, and exhibit a slightly steeper slope. In keeping with the trend exhibited by the tests at higher R ratios, the apparent propagation threshold was approximately 9 MPa$\sqrt{m}$. Below 8 MPa$\sqrt{m}$, early results indicate a dependence of the R ratio on near-threshold behaviour, i.e. an increase in the R ratio results in lower threshold values. For R = 0,8, $\Delta K_T \approx 7$ MPa$\sqrt{m}$ and, for R = 0,7, $\Delta K_T \approx 8$ MPa$\sqrt{m}$. Further tests are under way to confirm this. It should be noted, however, that the rates were maintained for several millimetres of crack growth.

Influence of temperature on growth rates

A comparison of the tests conducted at 20 and 290 °C with R = 0,1 is shown in Figure 8. It is apparent that, at 290 °C, higher growth rates, at least at ΔK levels below approximately 20 MPa$\sqrt{m}$, are obtained. This is most pronounced at about 8 MPa$\sqrt{m}$, with growth rates one order of magnitude higher than the results obtained at room temperature.

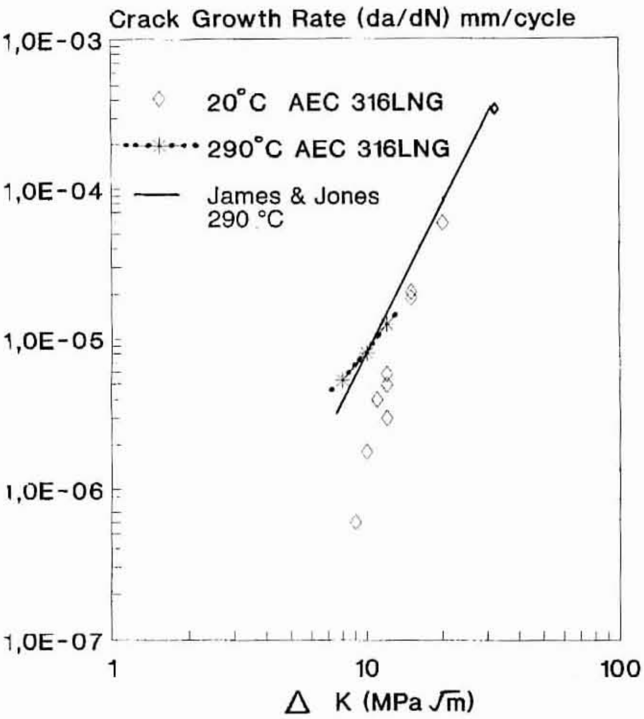

FIGURE 8. Effect of temperature on growth rates of cracks (R=0,1)

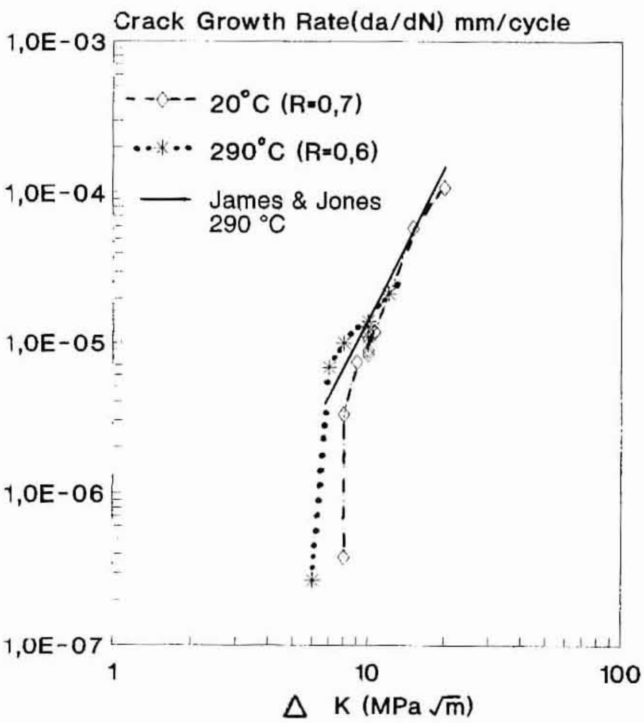

FIGURE 9. Effect of temperature on the growth rates of cracks

This appears to indicate that a lower threshold will be obtained at 290 °C. Further, it will be noted that the growth rates at 290 °C are in excellent agreement with the correlation developed by James and Jones[10].

As was the case for the low R ratio, the high-temperature growth rates at $R > 0{,}6$ differ from the trend developed at 20 °C (Figure 9). At 290 °C, the apparent threshold value is reduced from 8 MPa$\sqrt{m}$ to 5 MPa$\sqrt{m}$. Further testing is continuing. Once again, the correlation of James and Jones[10] provides excellent agreement at 290 °C.

Metallography and Fractography

Metallographic investigation revealed that the ASTM grain

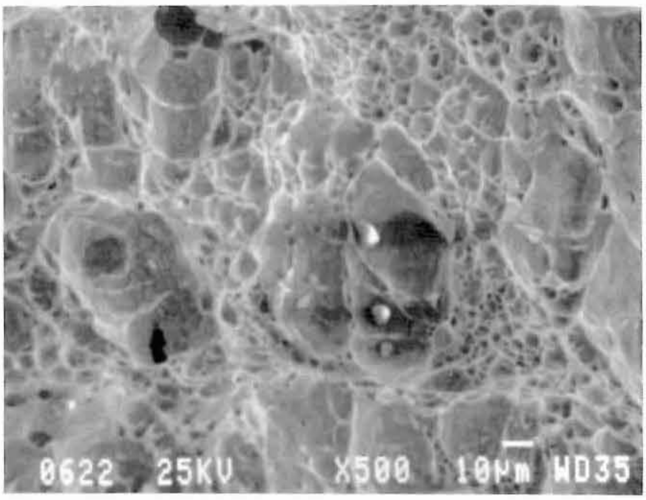

FIGURE 10. Non-metallic inclusions sparsely distributed within the fracture surface of 316LNG—ductile dimple failure mode

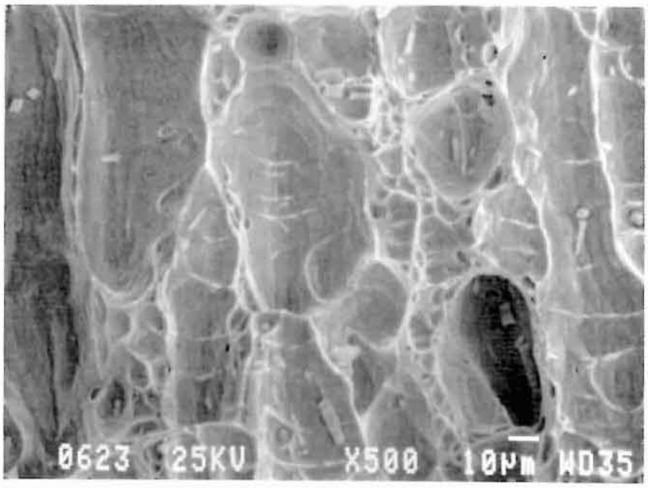

FIGURE 11. Fracture surface of commercial 316L

FIGURE 12. At low applied ΔK levels ($\Delta K < 10$ MPa$\sqrt{m}$), initiation occurred at single sites only. (AEC-316LNG 150 x magnification)

FIGURE 13. At higher delta-K levels ($\Delta K > 12$ MPa$\sqrt{m}$), multi-initiation is evident. (AEC-316LNG, 150 x magnification)

size of AEC-316LNG was 3 to 4, and that the material contained delta ferrite in the form of stringers elongated in the direction of the main working axis (circumferential). Typically, these were 10 µm thick and 100 µm long. Nonmetallic inclusions were spheroidal and sparsely distributed (Figure 10). EDAX analysis indicated that they were principally (Cr,Mn)S and (Cr,Fe,Mn)S. The fracture surface depicts ductile dimple failure. Figure 11 shows the fracture surface of a commercial 316L steel.

At low cyclic stress-intensity levels ($\Delta K < 10$ MPa$\sqrt{m}$), initiation occurred only at single sites (Figure 12) whilst, at higher levels ($\Delta K > 12$ MPa$\sqrt{m}$), multi-initiation was evident, as depicted in Figures 13 and 14.

In the tests at 20 °C, only transgranular failure was observed. No intergranular fracture occurred.

Conclusions

The following can be concluded from the work described here.

(1) The AEC-316LNG material has a very low susceptibility to sensitization. In all the simulated heat treatments examined in this study, no measurable sensitization was detected.

(2) Very similar crack-initiation characteristics to those of other 316 steels were observed for tests conducted at an *R* ratio of 0,1 and a temperature of 20 °C.

(3) Very similar initiation lives were obtained at 20 °C for material tested under *R* ratios 0,1; 0,6; 0,7; and 0,8.

(4) The apparent initiation threshold, defined as no growth at 2 million cycles, is slightly dependent on the applied *R* ratio. Increased *R* ratios result in lower threshold values.

(5) A reduction in initiation life of approximately 2 was measured when the test temperature was increased from 20 to 290 °C for specimens tested at an *R* ratio of 0,1.

(6) A marked reduction, approximately ten times, in initiation life was measured when the test temperature was increased from 20 to 290 °C for specimens tested with an *R* ratio of 0,6 or 0,7.

(7) The propagation behaviour of fatigue cracks at 20 and 290 °C exhibits a dependence on the *R* ratio at the same cyclic stress intensity. Higher *R* ratios ($R > 0{,}6$) result in higher propagation rates than at $R = 0{,}1$.

References

1. Atteridge, D.G., Bruemmer S.M., and Page, R.E. (1985). Evaluation of welded and repair-welded stainless steel for LWR Service. *NUREG report,* no. CR3613, vol. 2.
2. Sanderbergh, R.F. Evaluation of the degree of sensitization in type 316LNG, 304L, and 308/309 stainless steels. Laboratory for Materials Science and Metallurgical Engineering Incorporated (LMMI), report to the AEC.
3. Clarke, W.L., Romero, V.M., and Danko, J.C. (1977). Detection of sensitization in stainless steel using electrochemical techniques. Paper 180, Corrosion/77, San Francisco, NACE.
4. Devaux, J.C., D'Escatha, Y., Rabbe, R., Pellissier-Tanon, A. (1979). A criterion for analysing fatigue crack initiation in geometrical singularities. Transactions of the 5th International Conference on Structural Mechanics in Reactor Technology (SMiRT).
5. Saainouni, K., and Bathias, C. (1982). Study of fatigue crack initiation in the vicinity of notches. *Engineering*

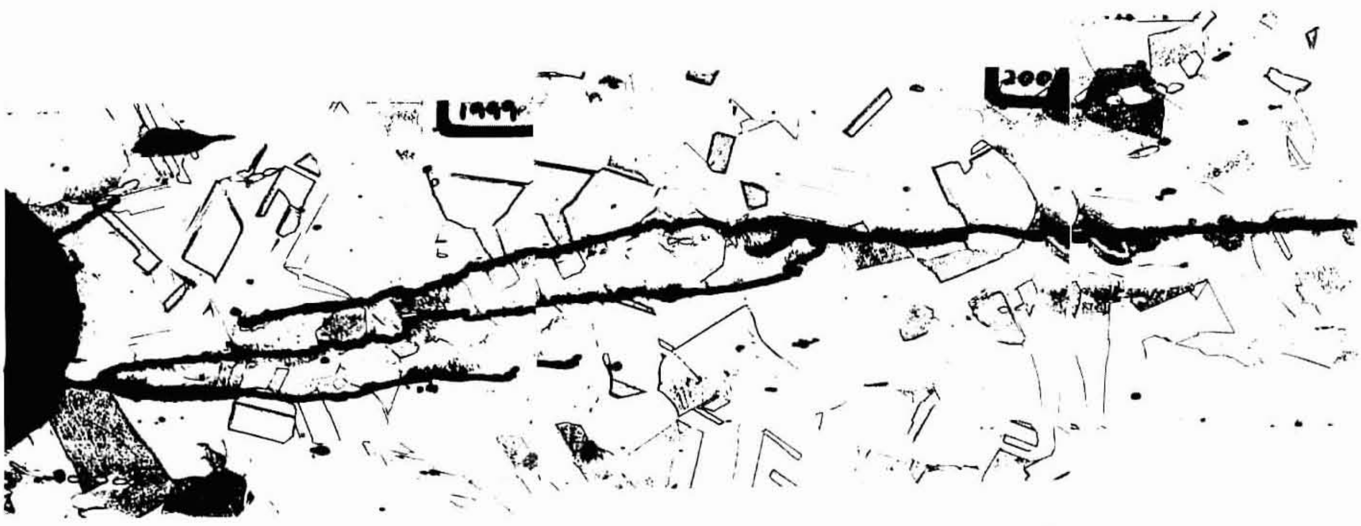

FIGURE 14. Multi-crack initiation sites typical of loading under high stress conditions ($\Delta K > 12$ MPa$\sqrt{m}$, AEC-316LNG)

Fracture Mechanics, vol. 16, no. 5, pp. 695–706.

6. Novak, S.R. (1983). Corrosion-fatigue crack initiation behaviour of four structural steels. *Corrosion fatigue: mechanics, metallurgy, electrochemistry and engineering.* ASTM STP 801, Crooker, T.W., and Leis, B.N. (eds.), American Society for Testing and Materials, pp. 26–63.
7. Braglia, B.L., Hertzberg, R.W., and Roberts, R. (1979). Crack initiation in a high-strength low alloy steel. *Fracture Mechanics,* ASTM STP 677, Smith, C.W. (ed.), American Society for Testing and Materials, pp. 290–302.
8. Barson, J.M., and McNicol, R.C. (1974). Effect of stress concentration on fatigue-crack initiation in HY-130 steel. *Fracture toughness and slow-stable cracking,* ASTM STP 559, American Society for Testing and Materials, pp. 183–204.
9. D'Escatha Y.C., Devaux, J.C., Bernard J.L., and Pellissier-Tanon, A. (1980). A criterion for analysing fatigue crack initiation in geometrical singularities. 4th International Conference on Pressure Vessels Technology, London, *Paper* C 34/80, pp. 211–222.
10. James, L.A., and Jones, D.P. (1985). Fatigue crack growth correlation for austenitic stainless steels in air. *Proceedings of the Conference of Predictive Capabilities in Environmentally-assisted Cracking.* Rungta, R. (ed.), PVP, vol. 99, American Society of Mechanical Engineering, New York, pp. 63–414.
11. Rickerby, D.G., and Fenici, P. (1984). Fatigue crack growth in thin section type 316 stainless steel. *Engineering Fracture Mechanics,* vol. 19, no. 4, pp. 585–599.